NASA's Soil Moisture Active Passive (SMAP) Observatory

Kent Kellogg
818-354-5386
Kent.H.Kellogg@jpl.nasa.gov

Sam Thurman
818-393-7819
Sam.W.Thurman@jpl.nasa.gov

Wendy Edelstein
818-354-8746
Wendy.N.Edelstein@jpl.nasa.gov

Michael Spencer
818-354-1175
Michael.W.Spencer@jpl.nasa.gov

Gun-Shing Chen
818-354-3375
Gun-Shing.Chen@jpl.nasa.gov

Mark Underwood
818-354-9731
Mark.L.Underwood@jpl.nasa.gov

Eni Njoku
818-354-3693
Eni.G.Njoku@jpl.nasa.gov

Shawn Goodman
818-354-6628
Shawn.D.Goodman@jpl.nasa.gov

Benhan Jai
818-393-7978
Benhan.Jai@jpl.nasa.gov

Jet Propulsion Laboratory, California Institute of Technology, 4800 Oak Grove Drive, Pasadena, CA 91109-8099

Abstract—**The Soil Moisture Active Passive (SMAP) mission, one of the first-tier missions recommended by the 2007 U.S. National Research Council Committee on Earth Science and Applications from Space, was confirmed in May 2012 by NASA to proceed into Implementation Phase (Phase C) with a planned launch in October 2014. SMAP will produce high-resolution and accurate global maps of soil moisture and its freeze/thaw state using data from a non-imaging synthetic aperture radar and a radiometer, both operating at L-band.**

Major challenges addressed by the observatory design include: (1) achieving global coverage every 2–3 days with a single observatory; (2) producing both high resolution and high accuracy soil moisture data, including through moderate vegetation; (3) using a mesh reflector antenna for L-band radiometry; (4) minimizing science data loss from terrestrial L-band radio frequency interference; (5) designing fault protection that also minimizes science data loss; (6) adapting planetary heritage avionics to meet SMAP's unique application and data volume needs; (7) ensuring observatory electromagnetic compatibility to avoid degrading science; (8) controlling a large spinning instrument with a small spacecraft; and (9) accommodating launch vehicle selection late in the observatory's development lifecycle.

TABLE OF CONTENTS

1. MISSION OVERVIEW AND CHALLENGES 1
2. MEASUREMENT APPROACH 2
3. INSTRUMENT DESIGN AND TRADES.....3
4. INSTRUMENT REFLECTOR-BOOM ASSEMBLY .6
5. RFI MITIGATION 8
6. SPACECRAFT DESIGN AND TRADES.....10
7. ADAPTING PLANETARY AVIONICS 12
8. EMI/EMC 13
9. INSTRUMENT ANTENNA CONTROL 14
10. LAUNCH VEHICLE CHALLENGES 15
11. LESSONS LEARNED 17
12. CONCLUSION.....18
REFERENCES.....18
BIOGRAPHIES.....19
ACKNOWLEDGEMENTS.....21

978-1-4673-1813-6/13/$31.00 ©2013 IEEE

1. MISSION OVERVIEW AND CHALLENGES

The Soil Moisture Active Passive (SMAP) mission (Figure 1) is one of the first Earth observation satellites being developed by NASA in response to the 2007 National Research Council's Earth Science Decadal Survey [1]. SMAP is currently in its implementation phase at NASA's Jet Propulsion Laboratory (JPL) [2] with support from the Goddard Space Flight Center (GSFC). The Project completed its Critical Design Review in July 2012, and will conduct its System Integration Review in April 2013. SMAP has a planned launch date in October 2014.

SMAP will produce high-accuracy, high-resolution global measurements of near-surface soil moisture and its freeze-thaw state. These measurements will greatly improve estimates of water, energy, and carbon transfers between the land and atmosphere [3]. The soil moisture control of these fluxes is a key factor in the performance of atmospheric models used for weather forecasts and climate projections. Soil moisture data are also key to assessing flooding and monitoring drought. Knowledge gained from SMAP's observations can help mitigate these natural hazards, resulting in potentially great economic and societal benefits. SMAP measurements will also provide high-resolution spatial and temporal mapping of the frozen or thawed condition of the surface soil and vegetation. Observations of soil moisture and freeze/thaw timing over the boreal

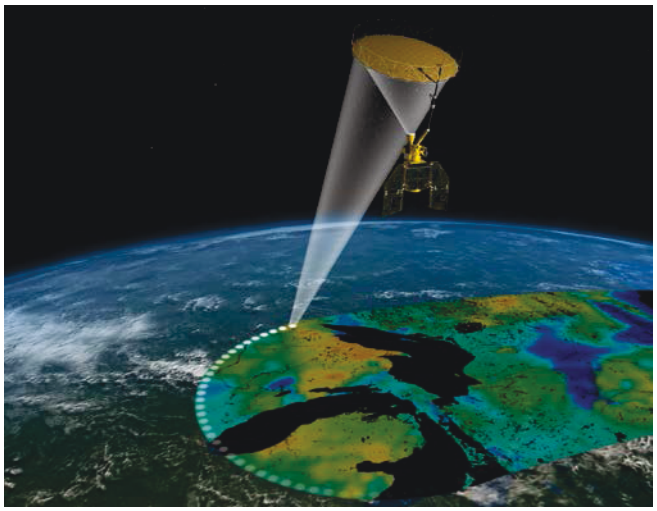

Figure 1. SMAP observatory launches in late 2014 to map soil moisture and its freeze-thaw state globally every 2–3 days.

latitudes will help reduce a major uncertainty in quantifying the global carbon balance.

SMAP's instrument combines a non-imaging (unfocused) synthetic aperture radar (1.26 GHz) and a digital radiometer (1.41 GHz) with a shared deployable, rotating, 6-meter offset-fed mesh reflector antenna [4]. The instrument is carried onboard a 3-axis stabilized spacecraft in a 685-km polar orbit with an 8-day repeating ground track. Instrument data allow high-accuracy global maps of soil moisture at 10-km resolution and freeze/thaw at 3-km resolution, every 2–3 days to be produced from algorithms applied in ground processing. The radar and spacecraft are being developed in-house at JPL, leveraging previous Earth mission radar experience and adapting power and avionics elements from a recent JPL planetary mission. The radiometer is being developed at GSFC leveraging previous Earth mission radiometer experience. Mission operations and science data processing will be conducted by JPL with GSFC support.

The measurement objectives pose unique challenges for the mission and instrument design:

- Achieving global coverage every 2–3 days with a single observatory;
- Achieving both high resolution and high soil moisture accuracy, including through moderate vegetation.

These challenges were addressed by the joint application of a radar and radiometer operating coincidentally at L-band with a shared conically scanning antenna that produces a 1,000-km-wide measurement swath, thereby enabling global coverage every 2–3 days with a single observatory operating in a sun-synchronous low-altitude Earth orbit (LEO).

Using L-band resulted in additional challenges for the instrument including:

- Accommodating the resulting large antenna size;
- Using a deployable mesh reflector antenna for L-band radiometric measurements; and
- Minimizing science degradation from L-band terrestrial radio frequency interference (RFI) common over many land areas.

The resulting instrument posed more design challenges:

- Concurrently developing and synergistically integrating new instrument and spacecraft system designs (collectively referred to as the "observatory") to reduce overall complexity and development effort;
- Adapting planetary heritage avionics to support high radar data rates and throughputs;
- Minimizing observatory-generated electromagnetic interference (EMI) that could degrade science data;
- Controlling the pointing and dynamic behavior of a relatively large spinning instrument and antenna with a comparatively small spacecraft bus; and
- Fault protection approach that also minimizes science measurement down-time on-orbit.

The launch vehicle selection process for SMAP involved both programmatic and technical challenges:

- Packaging the large instrument into a new observatory design compatible with several potential medium- and large-class launch vehicles; and
- Accommodating a final launch vehicle selection late in SMAP's design lifecycle without stretching the development schedule and delaying the launch date.

2. MEASUREMENT APPROACH

The instrument architecture and operating frequencies were confirmed early in Formulation. L-band was selected because of its unique advantages for soil moisture measurements. The atmosphere is relatively transparent, weather effects are acceptable, the intervening canopy wet and dry biomass is sufficiently transparent, and the soil emission is representative of moisture conditions to a significant depth beneath the surface. The L-band radiometry spectrum is protected for radio astronomy within the 1400–1427 MHz frequency range; however, even within this range sufficient leakage and unauthorized/unlicensed transmissions are present to necessitate incorporating RFI mitigation features into the radiometer and science processing system designs. The radar operates in shared spectrum as a secondary user; as a result, RFI mitigation is also needed for the radar.

SMAP's combined active (radar) and passive (radiometer) instruments enable high accuracy and high spatial resolution soil moisture measurements. The radiometer provides high soil moisture accuracy at moderate spatial resolutions (40 km) by measuring microwave emission from the soil; it is less sensitive to surface roughness and vegetation than the radar. The radar measures surface backscatter with high spatial resolution (1–3 km in high-resolution mode). The combined measurements can yield soil moisture with accuracy approaching radiometer-based retrievals and spatial resolution intermediate between that of the radar and radiometer. Thus, the driving aspects of SMAP's measurement requirements include simultaneous measurement of L-band brightness temperature and backscatter with a three-day revisit and spatial resolutions of 40 km and 3 km, respectively. The combined active/passive soil moisture product is produced at a 10-km resolution.

The conically scanning antenna and its size resulted from the confluence of several science requirements. Conically scanning antennas have been used on past missions (e.g., QuikSCAT) to achieve broad measurement swaths and efficient global coverage from polar LEO. The effects of vegetation and surface roughness are dependent on look

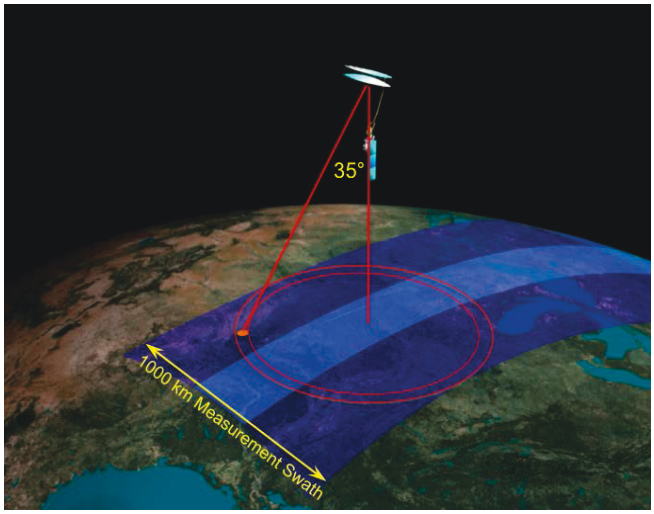

Figure 2. SMAP's conically scanning instrument has a 1,000-km swath that provides global coverage every 2–3 days.

angle and therefore, repeat measurements at the constant look angles provided by a conical scan approach greatly aids the retrieval of soil moisture. The choice of a constant incidence angle between 35 and 50 degrees reflects a trade between sensitivity to soil moisture, adequate separation in H and V polarization responses, and spatial resolution. The reflector's 6-m size was driven by the radiometer's real aperture resolution requirement (40 km). The 1,000-km-wide swath that results from this approach enables global coverage every 2–3 days (Figure 2).

Table 1. SMAP Instrument Requirements are derived from Science Measurement Needs

Scientific Measurement Requirements	Instrument Functional Requirements
Soil Moisture: ~±0.04 m^3m^{-3} volumetric accuracy in top 2–5 cm for vegetation water content ≤ 5 kg m^{-2}; Hydrometeorology at ~10 km; Hydroclimatology at ~40 km	L-Band Radiometer (1.41 GHz): Polarization: V, H, 3rd & 4th Stokes Resolution: 40 km Radiometric Uncertainty*: 1.3 K L-Band Radar (1.26 GHz): Polarization: VV, HH, HV (or VH) Resolution: 10 km Relative accuracy*: 0.5 dB (VV and HH) Constant incidence angle** between 35° and 50°
Freeze/Thaw State: Capture freeze/thaw state transitions in integrated vegetation-soil continuum with two-day precision, at the spatial scale of land-scape variability (~3 km)	L-Band Radar (1.26 GHz): Polarization: HH Resolution: 3 km Relative accuracy*: 0.7 dB (1 dB per channel if 2 channels are used) Constant incidence angle** between 35° and 50°
Sample diurnal cycle at consistent time of day (6 a.m. / 6 p.m.); Global, ~3 day revisit Boreal, ~2 day revisit	Swath Width: ~1,000 km Minimize Faraday rotation (degradation factor at L-band)
Observation over minimum of three annual cycles	Minimum three-year mission life

* Includes precision and calibration stability

** Defined without regard to local topographic variation

Table 1 summarizes SMAP's instrument requirements derived from science needs.

3. Instrument Design and Trades

Several candidate designs were considered for the instrument antenna, including a shared aperture electronically scanned phased-array, but only a reflector antenna simultaneously satisfied both radar and radiometer needs. Key drivers were operating frequencies, radiometer beam efficiency and noise performance, fixed incidence angle, and inertial properties to reduce spun momentum. A fixed rotation rate between 13 and 14.6 rpm ensures that adjacent footprints overlap by 30% with radiometer integration times and radar waveforms. The large aperture, mass properties, and launch vehicle packaging requirements drove the selection of a deployable mesh design. Such antennas have well-known flight heritage in fixed-pointing telecom applications from geosynchronous orbit, but this is the first known reflector that will be (a) flown in polar LEO and subject to periodic eclipse seasons; (b) in a continuously rotating measurement application; (c) supporting high accuracy L-band radiometric measurements; and (d) accommodated and controlled on a relatively small spacecraft. These requirements, the last three in particular, posed unique challenges for SMAP.

A key objective of the instrument design is to minimize spun momentum to enable the total observatory momentum to be managed by the spacecraft reaction wheels (rather than including a separate momentum wheel with its attendant control provisions as part of the instrument). To accomplish this, the radar electronics were placed on a spacecraft panel rather than with the rest of the spinning instrument. The radiometer was placed with the spinning antenna/feed to minimize radio frequency (RF) losses to radiometer (Figure 3).

L-band spectrum accommodation has been a particular challenge for SMAP. Heavy L-band spectrum usage creates a growing RFI challenge to both passive and active science sensors. In addition, proposed active science sensors must demonstrate that they will not interfere with terrestrial aircraft navigation systems that have priority in the active portion of the band. SMAP must be able to make accurate soil moisture measurements in the presence of significant terrestrial RFI. Based on experience and lessons learned from operating L-band sensors [5, 6], SMAP implemented several RFI mitigation techniques in the flight hardware and in the ground data processing to detect and remove RFI [7, 8, 9]. Furthermore, SMAP conducted significant tests and analyses, and made several revisions to the radar design, to ensure SMAP radar operation would not interfere with existing and planned Federal Aviation Administration (FAA) and Department of Defense (DOD) aircraft navigation systems [10, 11, 12]. Radar design changes included reducing pulse width (with increased peak power) and "hopping" the transmit frequency over the spectrum.

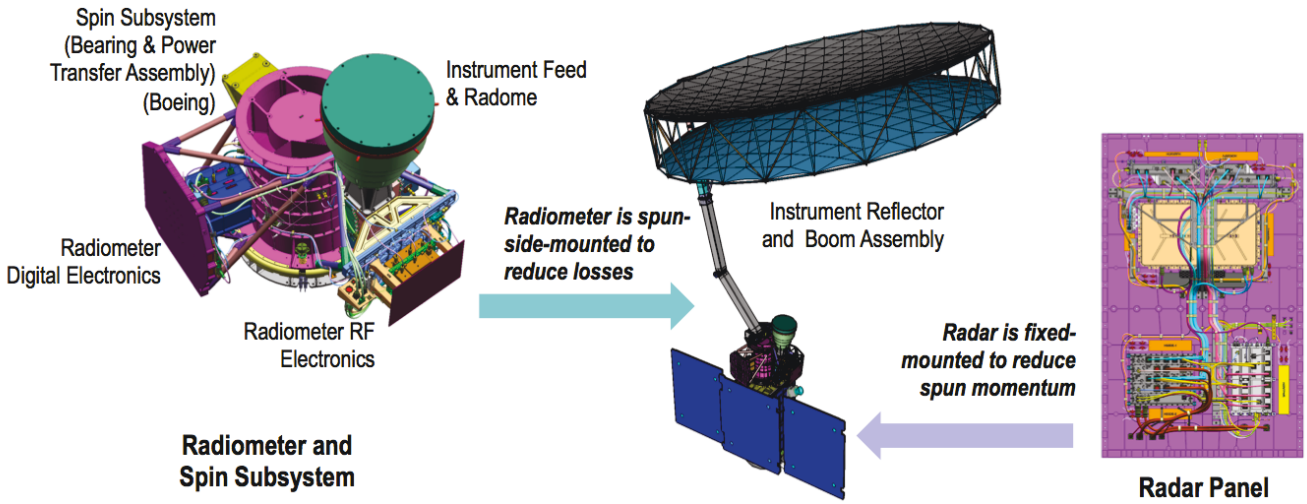

Figure 3. Instrument configuration and key assemblies.

The radar and radiometer operate continuously in a synchronous fashion. The radar transmits two polarizations sequentially at 2,850 Hz. The radiometer receives a synchronization signal from the radar and measures brightness temperature in-between the radar transmit events. The radar has two output data rates: high rate for synthetic aperture data and low rate for real aperture data. The radiometer also has two output rates: high rate for RFI mitigation and low rate for RFI quiet areas, such as over ocean (Figure 4). The radiometer and radar utilize a "state machine" field programmable gate array (FPGA)-based design approach with limited configurability. The instrument data rates are commanded by the spacecraft using a latitude/longitude based look-up table. The radar's 35 Mbps data rate places high data volume and data rate requirements on the spacecraft bus (up to 135 GB/day data return). Data volume requirements have been minimized by acquiring high-resolution data only on the descending orbit pass and only over land regions; this is all that is required to meet science requirements and greatly reduces the daily data volume compared with continuously returning high-resolution data. With this constrained data volume, SMAP is able to return its science data though NASA's Near Earth Network at X-band, and was thus able to avoid adding an additional high rate return link through NASA's Tracking and Data Relay Satellite System (TDRSS).

A simplified block diagram of the SMAP instrument is shown in Figure 5.

The radar is located on the fixed side of the observatory on the anti-sun spacecraft panel for thermal stability and relies on passive thermal control from the spacecraft. The RF electronics generates the radar chirps, amplifies, and transmits them to the rotary joint assembly that passes the RF signal to the feed horn and antenna. It also provides a stable calibration loop for gain calibration of the integrated transmit and receive paths. The calibration loop ensures calibration stability and repeatability over temperature. A single 500-W RF high power amplifier transmits radar pulses; a high power switch sequentially selects antenna polarization (H or V) of the transmitted pulse. The digital electronics command the radar and pass the down-converted echoes to the spacecraft non-volatile memory (NVM).

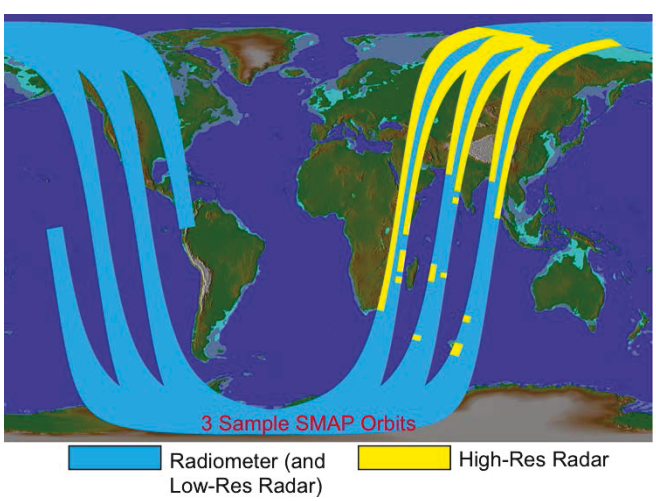

Figure 4. High-resolution (3 km) data is provided over land on the descending orbit pass and low-resolution (40 km) data is provided globally.

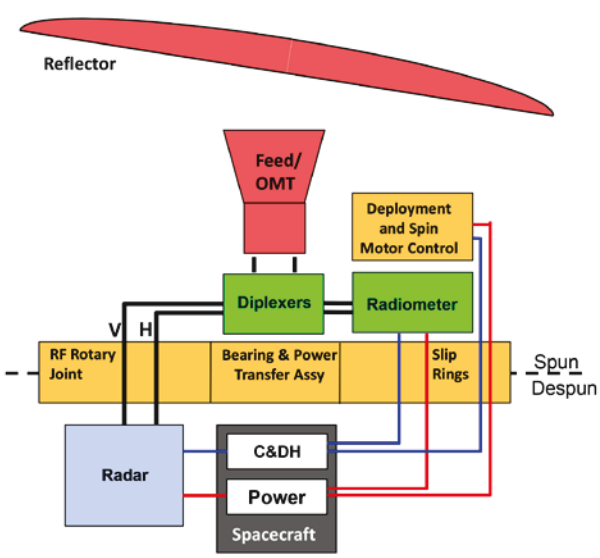

Figure 5. SMAP instrument block diagram.

Table 2. SMAP radar and radiometer requirements.

Parameter	L-Band Radar	L-Band Radiometer
Type	Synthetic Aperture Radar (non-imaging/unfocused)	Passive Microwave Radiometer
Frequency	1217–1298 MHz	1400–1427 MHz
Polarization	VV, HH, HV	V, H, 3rd, 4th Stokes
Accuracy	1.0 dB co-pol	1.3 K
Resolution	3 km	40 km
Data Rate	35 Mbps	4.3 Mpbs
Transmit Power	500 W peak, 9% duty cycle, 2850 Hz PRF*	N/A
RFI Mitigation	Frequency hopping over 1217–1298 MHz using 1 MHz/15 mu sec chirps	Spectral filtering

* Pulse Repetition Frequency

Digital filtering is used for narrowband detection at the tunable frequency for rejecting RFI. The radar is single string, but includes two RF receive channels, one for H and one for V polarizations. This provides a degree of graceful degradation because the loss of one polarization would degrade science but would not result in mission loss. Radar performance requirements are summarized in Table 2.

The radiometer measures microwave emissions for H and V polarization brightness temperatures, and provides 3rd and 4th stokes parameters that are used for RFI mitigation. The radiometer digital electronics includes digital spectral filtering for RFI mitigation. The key to high radiometric measurement accuracy is achieving repeatable, characterizable, and monotonic responses over temperature and time. Therefore, the thermal design employs passive design features for short-term stability, such as the use of a titanium thermal isolator and radome for the feed. In addition, active thermal control is used for additional seasonal stability, as well as for temperature set-point adjustment, which enables the operational temperature to be changed on-orbit to avoid gain non-linearities. This set-point feature was added to the design as a result of lessons learned from other microwave radiometer missions that exhibited this undesirable behavior. Radiometer performance requirements are summarized in Table 2.

A frequency diplexer allows the radar and radiometer to share a common instrument antenna. The diplexer simultaneously provides high RF isolation between the radar and radiometer frequencies and pre-select filtering for RFI rejection in a compact and low-RF-loss package. It also accommodates high-power handling capability for the radar.

The instrument antenna design is an offset-fed reflector arrangement (0.7 f/D) with a 6-m projected aperture and vertical and horizontal linear polarizations selectable through an orthomode transducer (OMT). Zenith deck mounting offered a number of system design and performance advantages including (1) lowest overall spun mass/inertia; (2) lowest RF transmission line losses to the radiometer and radar; and (3) lowest overall system noise temperature for radiometer measurements because most feed spillover 'sees' cold space. The zenith mounting location and conical scanning requirement, however, posed a significant constraint on the flight system design to avoid intrusions into the instrument antenna field of view (FOV) (the solar array design was a particular challenge). The zenith location also partially but significantly blocks visibility to the Global Positioning System (GPS)–this contributed to a decision in Formulation to forego on-board GPS capability for orbit position and ephemeris and to instead use Doppler tracking and ground-based time synchronization. The most significant design drivers on the antenna came from the radiometer: beam efficiency, reflector surface emissivity, and temperature knowledge to achieve antenna noise temperature requirements. Radar drivers on antenna performance were gain stability, sidelobes, and cross polarization levels. Key instrument antenna performance requirements are summarized in Table 3.

Mechanically, the spin subsystem and spun platform assembly provide the spin function; launch lock and release; mechanical support for the radiometer, feed and reflector-boom assembly (RBA); and spun-side electrical control functions (RBA deployment motors control, thermal control, telemetry, etc.). The heart of the spin subsystem is a Boeing-provided Bearing and Power Transfer Assembly (BAPTA) that includes the spin motor, bearings, 65 slip rings for power and digital telemetry transfer across the spinning interface, and the RF rotary joint used by the radar. The BAPTA is enclosed within the cylindrical instrument core structure that also provides the mounting platform for all spun-side assemblies. Integrated Control Electronics (ICE) control the RBA deployment motors, spun-side thermal control, and radiometer command and telemetry. The Radiometer Front-End Electronics and passive RF components such as the diplexer are mounted to the feed horn. The Radiometer Electronics and Spin Control Electronics are mounted to separate structures to optimize spun mass properties. A Cone-Clutch Assembly (CCA) is the structural interface between the spun platform assembly and the spacecraft, and also locks the spun platform and offloads the BAPTA bearings during launch. Design features are incorporated to attenuate pyroshock levels for the spun electronics and bearings.

Instrument mass and power breakdown is in Table 4.

Table 4. Instrument mass and power breakdown (reflects CDR estimates with growth contingency applied).

Instrument Subsystem	Mass	Power
Radar Electronics	56 kg	287W
Radiometer Electronics	40 kg	65W
Antenna (Feed + RBA)	79 kg	-
Spin Subsystem	41 kg	36W
Structure (includes thermal control and harnesses)	141 kg	59W
Total	**356 kg**	**448W**

Collectively, the instrument spinning elements form the Spun Instrument Assembly (SIA). The SIA is largely balanced, by design, by adjusting the antenna optical prescription, by appropriately offsetting the feed and spun electronics assemblies from the spin axis using varying strut lengths, and by including small pre-launch adjustable ballast/balance masses at key locations (mostly on the RBA) in the design. An aggressive mass properties management program insures that as-built spun-side mass properties are tracked; the pre-launch adjustable ballast/balance masses allow correction for as-built mass characteristics to ensure proper on-orbit balance is achieved. Extensive analysis and modeling of the system dynamics and control behavior demonstrated that robust and stable balance is achieved by the fixed instrument balance design approach coupled with the spacecraft pointing control authority. Practical SIA on-orbit adjustable balance mechanisms could only provide a small fraction of total available pointing margin and were therefore not included in the design. The spun momentum of the SIA is compensated by the spacecraft's reaction wheels and attitude control system (ACS). This arrangement simplified the instrument design as well as overall control and fault protection design for the observatory; however, it places a constraint on the maximum spun momentum of the SIA of 364 N-m-s (at CDR the estimated spun momentum was 326 N-m-s). Another instrument configuration benefit is that most of the spun mass is concentrated near the rotation axis, which greatly reduces the sensitivity of spun momentum to mass growth.

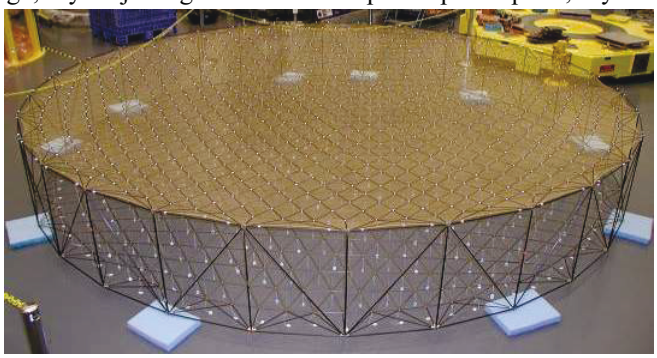

Figure 6. 5-meter AstroMesh™ Lite engineering model reflector (NGAS - Astro Aerospace).

4. INSTRUMENT REFLECTOR-BOOM ASSEMBLY

The 6-m shared reflector posed a number of unique challenges for SMAP:

Table 3. SMAP instrument key antenna requirements.

Key Requirement	Description
Antenna type	Offset-fed deployable parabolic reflector
Projected aperture	6 meter
Focal length	4.2 meter (f/D = 0.7)
Antenna gain	>35.5 dBi (radar)
Gain stability	<0.07dB (radar)
Sidelobe level	<-45 dB in nadir direction (radar)
Integrated cross pol	<-18 dB (radar)
Beamwidth	<2.8° for radar; <2.5° for radiometer
Main beam efficiency	>87% (radiometer)
Antenna temperature	<0.5 K° (radiometer)
Reflector emissivity	<0.0035; <.001 knowledge (radiometer)
Reflector temperature knowledge uncertainty	<60°C (radiometer)
Pointing	35.5° from spin axis; <0.02° knowledge
Reflector surface	20 OPI*, gold-plated molybdenum mesh
Feed type	Waveguide feed & OMT (WR-650)
Radome	Expanded Polystyrene (EPS)

* Openings-per-inch

- Packaging and deployment to accommodate fairing volume and spacecraft constraints;
- Spinning and pointing control of such a structure;
- Use of a mesh deployable for radiometric measurements; and
- Accurate pre-launch RF pattern characterization, accounting for spacecraft interaction effects.

Northrop Grumman Aerospace System's (NGAS) deployable Astromesh™ (AM) reflector was selected and its mass properties are ideally suited for SMAP's application [13]. These reflector designs have been used in geosynchronous communications satellite applications including Thuraya, Mobile Broadcasting Satellite (MBSAT), Inmarsat-4, and Alphasat. SMAP uses a derivative of Astro's heritage antenna design, AM-Lite (Figure 6), which accommodates smaller aperture sizes and fits within a smaller stowed volume. This is the first known application of this kind of deployable reflector design within a high-performance microwave radar and radiometer antenna system, operating in LEO and also in a spinning configuration. Each of these 'firsts' poses unique challenges for SMAP that have been addressed within the mission and system design, and in the verification and validation (V&V) approach. The overall configuration and basic components of the stowed and deployed reflector are shown in Figure 7.

The reflector uses a perimeter truss consisting of composite tubes to support front and rear webs of fiber-reinforced tape. The reflector surface is a 20-OPI, gold-plated molybdenum wire mesh held in place with a net that attaches to a front web to provide the proper spacing to form the mesh's parabolic shape. The perimeter truss is attached to a prime batten, which in turn attaches to the two-segment boom. The boom is made of two graphite/epoxy tubes connected by hinges that allow the furled reflector to be stowed for launch to fit within the launch vehicle fairing. Pyro-initiated

releases are required to open launch restraints before the boom can be deployed.

RBA deployment is a significant driver to the mission and observatory design. The boom and reflector are deployed separately (boom first, followed nominally by the reflector two days later). The LEO orbit drove the thermal designs to ensure there were no "hot spots" that could either overheat or introduce large thermal gradients, which could add deployment risk. An operational constraint is imposed to idle spacecraft guidance and attitude control during deployment to eliminate ACS reaction loads on the RBA. This, in turn, places requirements and constraints on the deployment duration to be completed within 40 minutes (a spacecraft power constraint). Heritage reflectors have been deployed over long periods (hours) to prevent motor overheating, so new motor and thermal designs were required for SMAP to accommodate the short deployment time and thermal loading.

The <0.5 K° radiometer antenna temperature calibration requirement places challenges on the mesh and web RF emissivity and mesh temperature knowledge (mesh emissivity <0.0035, mesh emissivity knowledge to 0.001, mesh temperature known to 60°C). Early measurements of mesh materials were completed to confirm it was acceptable for soil-moisture applications (Figure 8). Mesh density (OPI) was assessed to meet L-band emissivity requirements. 20 OPI was selected as the best trade between mass properties and RF performance (lower mass and easier to stow and manage than 40 OPI density, and although the 10 OPI mesh has lower mass it was found to be too lossy for L-band radiometer measurements). Mesh temperature knowledge is another key parameter required for antenna pattern correction. Mesh temperature cannot be measured directly on-obit, so it will be determined by ground test-verified models to provide on-orbit temperature estimates.

Figure 8. Mesh emissivity test setup and sample.

Heritage reflectors have been flown in geo-synchronous orbits. The LEO environmental effects on the mesh had to be considered during the mesh qualification, including effects of the extensive thermal cycling on-orbit, effects of atomic oxygen, solar ultraviolet (UV) radiation, electrostatic discharge (ESD) charging, solid particles, and passive intermodulation (PIM) concerns. The mesh qualification program determined that "cold welding" from thermal cycling or gold flaking due to CTE mismatch were not credible failure modes. The mesh is not susceptible to oxidizing from the atomic oxygen. The RF performance would be negligibly impacted if there were a small hole or tear in the mesh from a solid particle micrometeroids. PIM was determined not to cause an interference concern for science or telecom functions. In communication applications of the mesh reflector, the webs are typically painted with a conductive paint for ESD considerations. However, for SMAP, this type of paint contributed too much radiometric loss and had a significant impact in the overall antenna error budget, so an effort was made to eliminate the use of the paint. However, it was determined that the un-painted webs would degrade unacceptably in the vacuum UV environment, so a paint was ultimately selected that was both low loss and tolerant to atomic oxygen and UV. This is an example of how critical RF performance had to be carefully balanced with other design considerations such as operating in LEO.

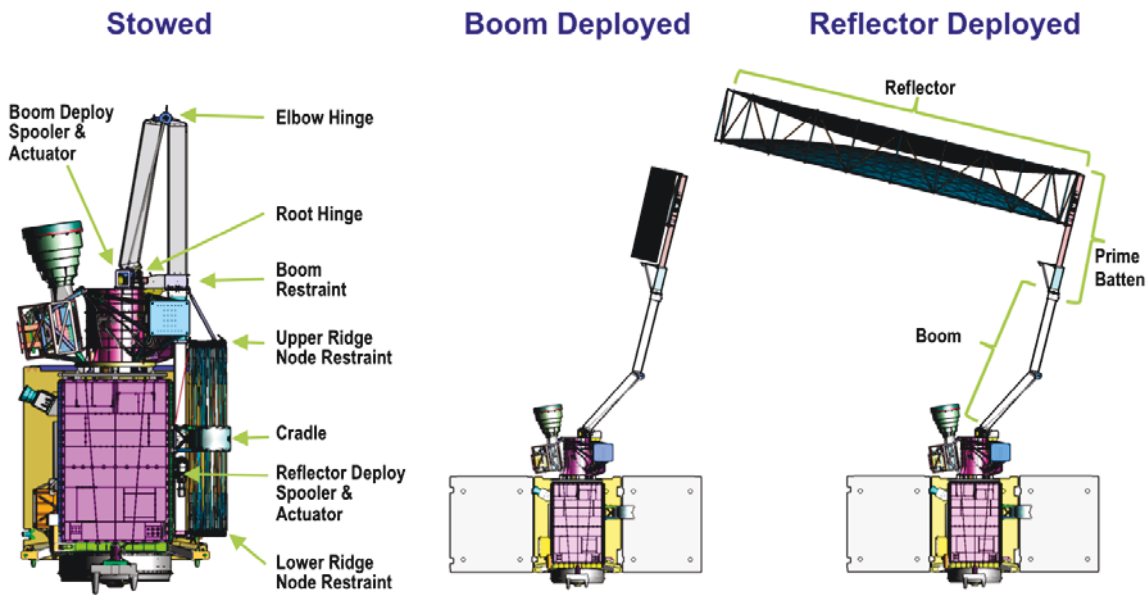

Figure 7. SMAP's reflector-boom assembly stowed and deployed configurations.

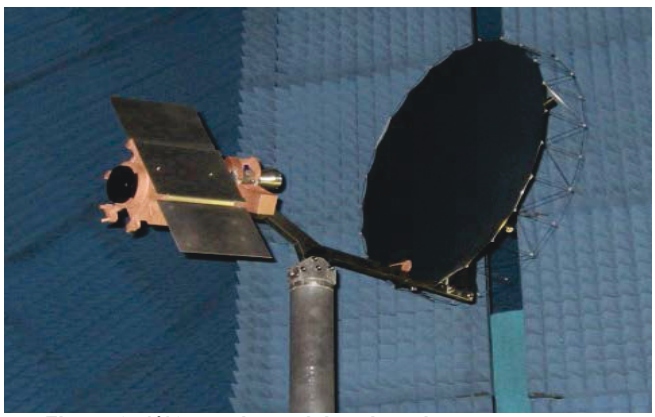

Figure 9. 1/10th scale model undergoing antenna range measurements.

Another challenge related to the RBA has been the extensive modeling and component level testing for a piecewise verification of the antenna RF performance. Radar and radiometer performance are highly dependent on antenna pattern characteristics such as gain, half-power beamwidth, sidelobe and cross-polarization levels, and electrical pointing. SMAP's large antenna size and gravity effects make it impractical and high risk to conduct an end-to-end antenna test on the ground in a flight-like configuration and environment (to "test as you fly"). The antenna pattern RF performance is being verified by a combination of test and analysis. Scattering from the boom, solar panels, and other parts of the observatory structure affect the antenna pattern. Moreover, the radar and radiometer have stability requirements for pattern characteristics. GRASP™ is used to model the antenna in the presence of the observatory to determine the effects that could change the antenna pattern, such the FOV changes as the antenna rotates, reflector and boom thermal distortions, and dynamic distortions from spacecraft. As an independent verification, a high-fidelity 1/10th scale model of the observatory was tested to confirm the GRASP™ model (Figure 9). The flight feedhorn pattern characteristics will be measured and applied to the GRASP™ RF model to form the final-prelaunch antenna performance. The performance will be verified and uncertainties will be refined during post-launch commissioning and during the science calibration and validation campaign.

5. RFI MITIGATION

The L-band spectrum region (Figure 10) is heavily used and SMAP's measurements are made over land areas, where most potential interferers are located. This contrasts with the similar L-band Aquarius mission, where the primary target is the relatively RFI-quiet ocean. It's also worth noting here that RFI is evolving and generally increasing over time and that trend is expected continue into the future; SMAP must therefore be prepared to operate not only in the RFI environment as it exists today, but also in the RFI environment that may exist later in this decade. To meet radiometric accuracy requirements, SMAP has adopted aggressive measures to identify and mitigate the effects of RFI. Because SMAP is a global mapping mission with continuous, near-real-time generation of data products, any RFI mitigation techniques must lend themselves to reliable automation in ground processing software. The nature of the RFI threat differs somewhat for the radiometer and radar channels, which are treated in turn.

Radiometer

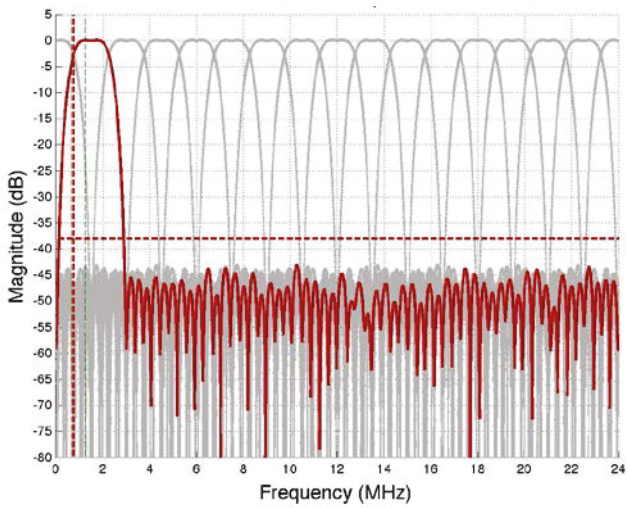

Figure 11. Radiometer band divided into 16 x 1.5 MHz spectral sub-bands for RFI detection.

RFI power in the radiometer's 24 MHz bandwidth will positively bias the observed brightness temperature, resulting in an erroneous dry bias in soil moisture estimates if uncorrected. While large RFI impacts (> ~40–50 K) can be detected and discarded, causing data loss, smaller RFI contributions are more difficult to detect and more likely to impact science product accuracy. Errors resulting from RFI corruption of even ~0.5 K are significant, therefore the radiometer includes a digital receiver to enable RFI detection and mitigation [7].

An extensive effort has been conducted to characterize the RFI environment expected for the radiometer. Two primary sources of RFI information have been utilized: a set of airborne observations in the United States and observations from European Space Agency's (ESA) Soil Moisture and Ocean Salinity (SMOS) L-band radiometer. Results show a variety of sources are present, including pulsed and narrowband, with some limited evidence of "broadband" continuous sources. SMOS data do not provide detailed RFI source information, but do provide a global characterization of observed RFI power levels. In particular, SMOS data

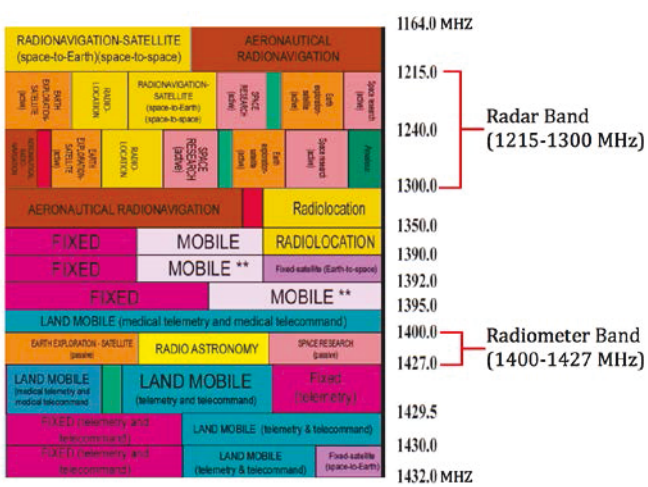

Figure 10. SMAP radar and radiometer operate within congested spectrum allocations that require RFI mitigation strategies to be applied.

show increased RFI levels in global regions outside the Americas [5].

Available characterization data shows RFI sources are either pulsed or narrow-band [i.e., continuous wave (CW)–like] in nature. Pulsed sources can be detected in the time-domain if the radiometer detector is sampled at a sufficiently high temporal resolution. The radiometer has a fundamental sampling frequency at the radar PRF of 3.2 kHz, which allows ground-based sub-millisecond RFI detection and mitigation using simple time-domain pulse thresholding strategies. To detect and mitigate CW sources, the radiometer's 24 MHz bandwidth is digitally filtered into 16 × 1.5 MHz sub-bands (Figure 11). Detected powers in these sub-bands will be telemetered to the ground at ~ 1 msec temporal resolution. The resulting ~ 1.5 MHz × 1 msec spectrogram dataset can be utilized in a variety of RFI detection methods, including channelized pulse detection, cross-frequency algorithms, or "peak-picking" methods.

In addition to time/frequency discrimination, the radiometer digital subsystem will also compute the first through fourth moments of observed fields both in the 24 MHz "full-band" (i.e., 3.2 kHz) and 1.5 MHz "sub-band" (16 channel × 1 msec) datasets. The availability of these moments will enable computation of the full-band and sub-band kurtosis [14] for RFI detection, which has also been shown effective against several source types.

Radar

In contrast to the radiometer, the SMAP radar operates in a "shared" band between 1215 and 1300 MHz with other services including FAA and DOD aircraft navigation systems. Very strong interference from these systems is expected, and indeed has been observed by previous L-band radar missions. Most potential interfering emissions at L-band are relatively narrow band. Because the SMAP radar itself is a narrow band system (1 MHz linear chirp), a key RFI avoidance strategy for SMAP is to make the center transmit frequency adjustable. If persistent RFI is encountered in a given band over a given region, the center frequency is simply commanded to a different location in the spectrum. Despite best efforts to operate the SMAP radar in a "clear" band, however, it is inevitable that some RFI contamination will be observed. Therefore, RFI detection and removal will be performed as part of ground data processing.

As with the radiometer, an extensive effort has been made to characterize the RFI environment expected for the radar. An examination of currently operating L-band systems indicates that 87% of RFI is from "pulsed" sources, and 13% is from "other" sources such as CW emitters. A simulation, developed to model RFI and the effectiveness of mitigation algorithms, uses the database of known emitters over North America. RFI emitter characteristics are varied in different runs of the simulation to assess sensitivities. To validate the RFI simulation, it was run assuming the Aquarius instrument parameters and orbit. When compared against the actual Aquarius data, the agreement was found to be excellent (Figure 12). In order to estimate the impact of

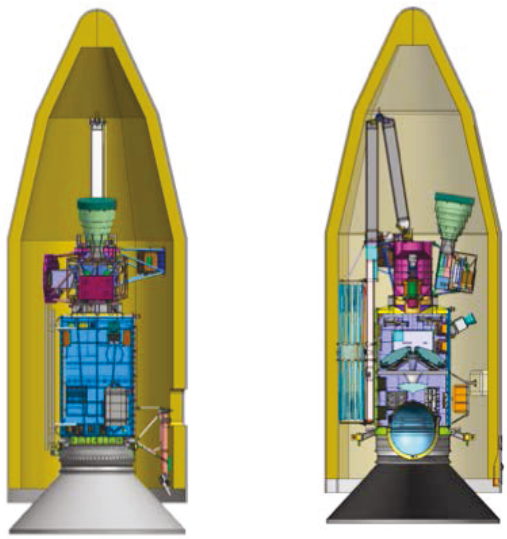

Figure 13. The Minotaur IV 92-inch fairing posed the largest constraint on the observatory packaging design.

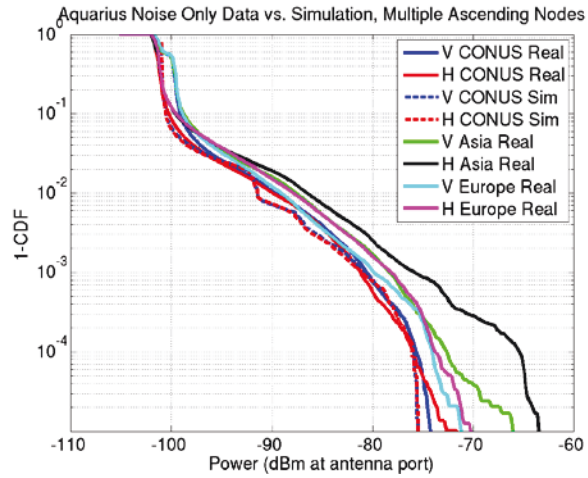

Figure 12. Complementary cumulative distribution functions of real and simulated Aquarius radar noise-only data for sets of passes over different geographical regions. Power levels above the radar noise floor are due to RFI.

other regions of the world where the RFI is observed to be somewhat worse (e.g., Europe and East Asia), the simulation can be run with an increased number of emitters, with higher duty cycles, higher powers, etc.

The primary detection/correction algorithm for pulsed interferers is Slow-Time Thresholding (STT) [15, 16]. Here, the fact that the PRF of RFI signals is usually slow relative to the SMAP PRF is leveraged. The STT technique looks at the slow-time series associated with a given range bin, sets an appropriate threshold, and flags any azimuth samples that exceed this threshold as RFI events. When the STT is applied to the results of the North American simulation described above, it is observed that the overall measurement errors due to RFI will be well within the budgeted allocation of 0.4 dB RMS. Further, this mitigation technique appears robust to artificially intensifying the RFI environment in the simulation to approximate regions other than North America.

6. Spacecraft Design and Trades

As discussed above, the spacecraft design was developed concurrently and synergistically with the instrument to reduce overall observatory complexity and therefore, development effort. Spacecraft development addressed the unique challenges associated with instrument accommodation and implementation approach. Planetary avionics from a previous JPL mission were adapted to support SMAP's high data volume and data rates, and also to support the high degree of functional integration between the instrument and spacecraft. In addition, the spacecraft was required to maintain compatibility with several launch vehicles including the Minotaur IV+, Atlas V, Falcon 9, and most recently the Delta II until relatively late in the design lifecycle without slowing the development or delaying the launch ready date (the Delta II was selected by NASA for SMAP at CDR-time). From the spacecraft and observatory packaging and volume standpoint, a key challenge was packaging the RBA within the most constraining vehicle: Minotaur IV+ with the 92-inch fairing (Figure 13). Designing for electromagnetic compatibility was also a challenge given the sensitivity of the instruments (and especially the radiometer) to L-band emissions. The RBA and SIA also posed a challenge to the spacecraft's pointing control design. This also posed a challenge for the fault protection design, primarily to ensure that minor faults do not result in a spin down of the observatory with the additional loss of science observation time that would impose.

The spacecraft is three axis–stabilized and employs momentum compensation via reaction wheels to accommodate the angular momentum of the spinning instrument. The spacecraft has an aluminum primary structure with a zenith deck provided for mounting the SIA and an anti-sun facing panel for mounting the radar electronics. A modular design for accommodating subsystems, each on a panel, provides for ease of integration (Figure 14). A deployable, fixed solar array with three panels is utilized as the primary power source and provides about 1400 W for the observatory. The secondary battery is a single 74-Ah capacity Li-ion small cell battery based on NASA Aquarius/ Argentina's/CONAE Satélite de Aplicaciones Científicas-D (Satellite for Scientific Applications or SAC-D) and Kepler spacecraft heritage. SMAP employs a high heritage blow-down monopropellant hydrazine (N_2H_4) propulsion subsystem composed of eight 4.5-N dual valve MR-111C thrusters and a single ROCSAT-heritage titanium diaphragm fuel tank.

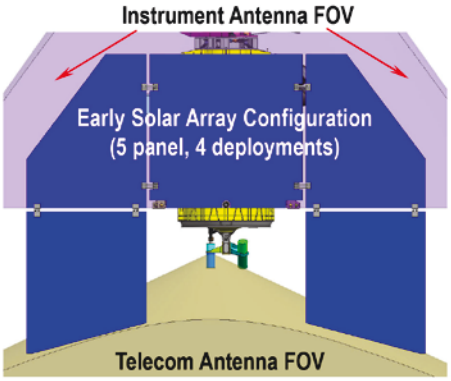

Figure 15a. Early solar array configuration was constrained by both instrument and telecom antenna FOVs.

SMAP spacecraft avionics and power electronics leverage a JPL planetary heritage design based on the commercial RAD750 flight computer and Peripheral Component Interconnect (PCI) bus architecture for the Command and Data Handling subsystem (C&DH), 1553 data bus as the observatory command and telemetry backbone, built-to-print design for telecommunication and instrument interfaces, power bus architecture (including power converters, switches, and pyro-firing circuits) for the Power and Pyrotechnic subsystem, as well as the control electronics for the Reaction Control System (thrusters and latch valves). A small number of new capabilities were added, including a 128 GB NVM capable of accommodating much larger science data storage volumes and transmission rates (130 Mb/s downlink rate vs. 6 Mb/s typical for planetary missions' maximum X-band downlink rate), new engineering interface control, a high-capacity solar array interface, and a new power bus controller.

The ACS employs high-heritage, flight-proven attitude sensors and control mechanisms. Attitude knowledge is provided by a star tracker and 12 sun sensors, which also support safing and attitude reinitialization. Redundant inertial measurement units propagate attitude knowledge between stellar attitude updates. Three large reaction wheels, with a 4th wheel used for momentum compensation, maintain momentum balance between the spacecraft and the SIA and counteract any disturbance torques. Three magnetic torque assemblies are used to manage the reaction wheel momentum and are controlled based on on-orbit magnetic field information from a single 3-axis magnetometer. Orbit position is determined via two-way Doppler tracking and propagated on-board the spacecraft.

The telecom subsystem is composed of redundant S-band transponders for uplink/downlink command and telemetry functions to the NASA Earth Network and Space Network (single access mode). The transponder provides for coherent Doppler tracking to support orbit determination. The high rate X-band data downlink is provided by redundant X-band transmitters. As stated earlier, science data volume was sufficiently constrained to enable science requirements to be met without requiring a TDRSS data return capability. The telecommunication antennas are mounted on a fixed (non-deployable) outrigger at the nadir end of the spacecraft.

The solar array deployed geometry and configuration was constrained to avoid intrusion into the instrument antenna RF FOV from the zenith direction and to avoid intrusion into the nadir-mounted telecom antenna FOV. Several solar array configurations evolved before final design selection (see evolving configurations in Figures 1, 2, 3, and 15). Early in development, solar array size was maximized (within the above FOV constraints) to avoid potential power constraints elsewhere in the design–this in turn drove a five-panel configuration with four separate deployments (Figure 15a). Later, as power requirements matured, the solar array was simplified to a three-panel configuration (with only two

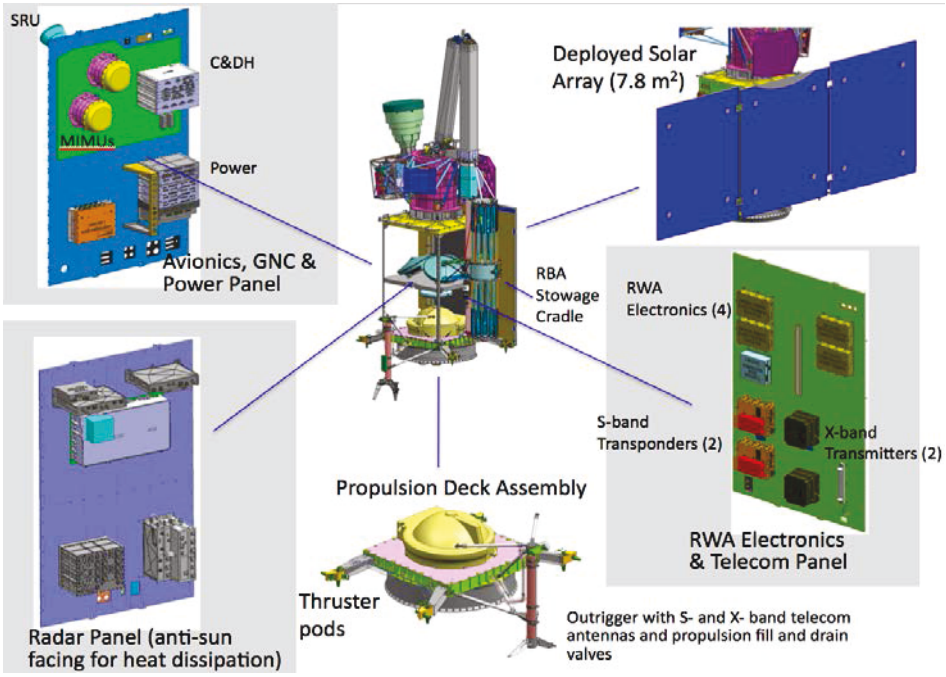

Figure 14. SMAP employs a modular packaging approach.

Table 5. Observatory mass and power breakdown (reflects CDR estimates with growth contingency applied).

System	Mass	Power
Instrument (from Table 4)	356 kg	448 W
Spacecraft (dry)	686 kg	903 W
Propellant	80 kg	-
Total	**1122 kg**	**1351 W**

deployments) that protruded slightly into the instrument antenna FOV (Figure 15b). The resulting RF pattern and performance perturbations from the intrusion can be removed in ground science data processing; however, high-fidelity RF analysis (confirmed by scale model testing) showed that perturbations are very minor and may be negligible. The stowed configuration was also significantly driven by launch vehicle fairing packaging and resulted in having no exposed cells when stowed. This iterative design example is representative of the close interaction between science, instrument, and spacecraft design teams to arrive at the least complex design to satisfy mission requirements.

SMAP uses a single-string architecture with selective redundancy. Graceful degradation features have also been designed into the observatory where practical. The transponders, transmitters, and inertial reference units (IRUs) are redundant. Propulsion latch valves are mounted in parallel for redundancy and all the thrusters are placed on a single branch. The reactions wheels are oriented and sized so that a failure in an individual wheel can be tolerated. Each magnetic torque assembly is internally redundant (via redundant windings) and magnetic field information can be provided via a ground-based model in the case of a magnetometer failure. Survival heaters and many instrument slip rings are redundantly wired. All actuators include redundant windings.

Particular attention has been paid to fault protection design to reduce the likelihood and mission impact of specific faults and also to minimize the number of fault events that cause the instrument to despin. The observatory is designed to robustly and autonomously recover attitude following the momentum change associated with a despin, but the return to science operations is a longer process resulting in undesirable science data loss. For this reason, the instrument remains spinning for all but the most severe faults (Figure 16).

Observatory mass and power breakdown is in Table 5.

7. Adapting Planetary Avionics

SMAP's avionics design is derived from the Mars Science Laboratory (MSL), a much more complex mission than SMAP. SMAP's challenge was to selectively apply elements of MSL's design to avoid unnecessary complexity for SMAP's application while also minimizing the amount of new design and development required. In the end, SMAP was able to substantially reduce the hardware complement relative to the MSL design and also limit the number of new board designs required. Another challenge was to adapt MSL's fully redundant design to a single string application.

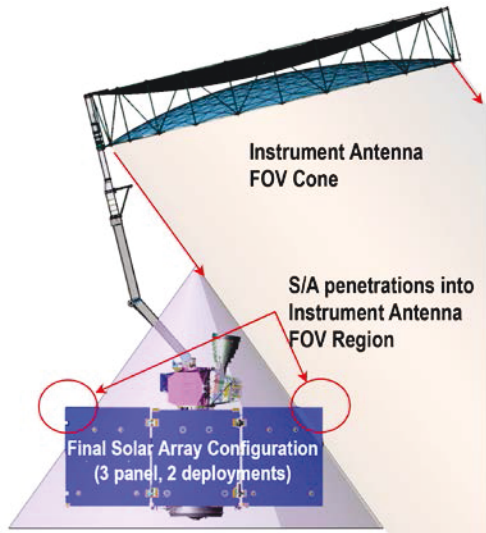

Figure 15b. Final solar array simplified to reduce panels and deployments; allowed slight penetration into instrument antenna FOVs.

To minimize new avionics development, the most significant capability changes were addressed by the development of the NVM card. Specific challenges that this card addressed were (1) managing simultaneous high rate read/write capability to support simultaneous science acquisition (6 Mbps for radiometer and 40 Mbps for radar) while also conducting downlink operations (130 Mb/s) within a single card; (2) high volume science data storage (128 GB); and (3) radiation fault tolerance/low bit error rates (BER) (10^{-9}) to prevent science data loss. The NVM leveraged a similar architectural design developed for the MSL MastCAM instrument; however, the MSL NVM only had 4 GB storage and a 6 Mbps transport rate. Using the NVM avoided adding a separate solid state recorder within the bus, which would have proved difficult to package given the volume constraints. The new NVM card is

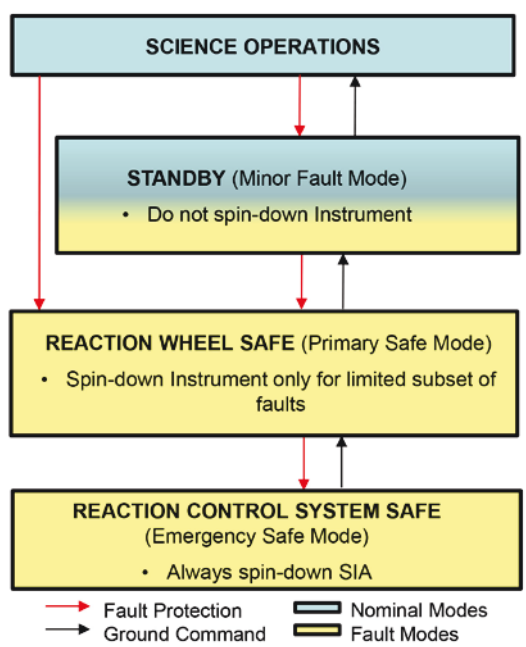

Figure 16. SMAP observatory fault protection is designed to reduce faults that spin down the instrument.

shown in Figure 17.

A new 128 GB flash memory chip was selected for the NVM, with a layout compatible with the older chip used in MSL's NVM card design. A large lot of these new parts was procured early in Formulation and subjected to extensive environmental, radiation, and life qualification testing. Test results showed that the actual BER performance was orders of magnitude better than required for the SMAP application [17]. This, in turn, enabled SMAP to implement the NVM with a relatively simple error detection and correction approach rather than a more complex approach recommended by the manufacturer for other applications. Beyond the mission-specific results for SMAP, the work conducted to qualify these parts contributed to the recently published Flash Qualification Guideline for Space Application [18]. Early testing on an MSL EM MASTCam NVM card showed the data throughput capability to be 130 Mb/s. SMAP set this as a constraint on the maximum downlink science data rate to avoid further significant design effort associated with this card. Further design refinements during development yielded improvements in data throughput; the engineering model NVM demonstrated a 280 Mb/s throughput capability, providing significant margin over SMAP's requirement.

8. EMI/EMC

Great attention was given in the design of the observatory for EMC with all the expected electromagnetic environments including the self-generated environments. Observatory radiated emissions could adversely affect radiometer science performance; therefore, the most severe EMC requirement limits (notches) are on those emissions in the radiometer band (Figure 18). There are less stringent notches at specific frequency ranges to protect the radar, transponder and launch vehicle systems.

During Formulation, SMAP established an EMC Design Control Plan [19] to provide design guidance to ensure requirements compliance. New designs incorporated best practices to reduce the likelihood of generating L-band emissions. In electronics, clock transitions were slowed and grounding paths were made as short as practical. Energy generated that could become radiated is contained within a complete Faraday cage created by sealed electronics boxes and shielded cabling. The spacecraft structure could not be an adequate Faraday cage due to the large number of penetrations required.

Electronics boxes were fabricated without joints where possible; close-outs were sealed with EMI gaskets or EMI tape. Assemblies that were constrained to use high-density D-connectors that leak emissions at L-band were treated with conductive overwrap to provide a complete covering. Pedestals for connectors on the C&DH assembly were added to aid overwrap application, and a cover plate was added to seal the gaps between faceplates of the individual cards in the box (Figure 19).

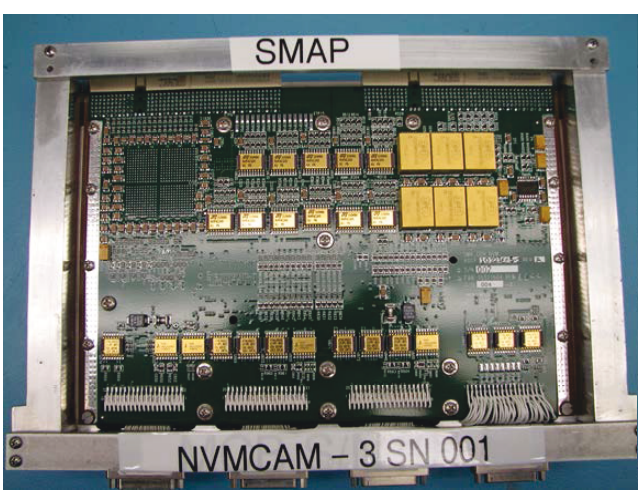

Figure 17. New NVM card for SMAP.

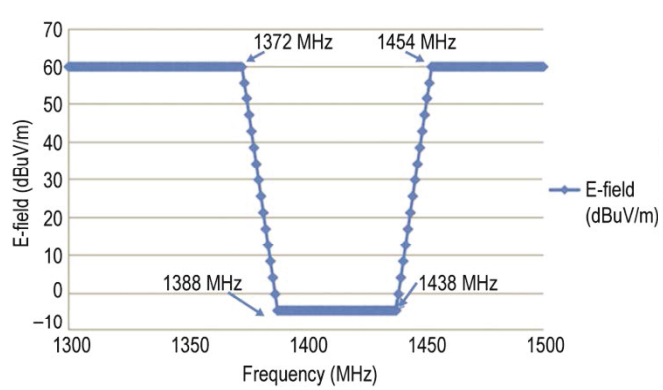

Figure 18. EMC requirement in the radiometer band for assemblies outside the spacecraft structure. Inside the structure, the lower limit is relaxed by 6 dB.

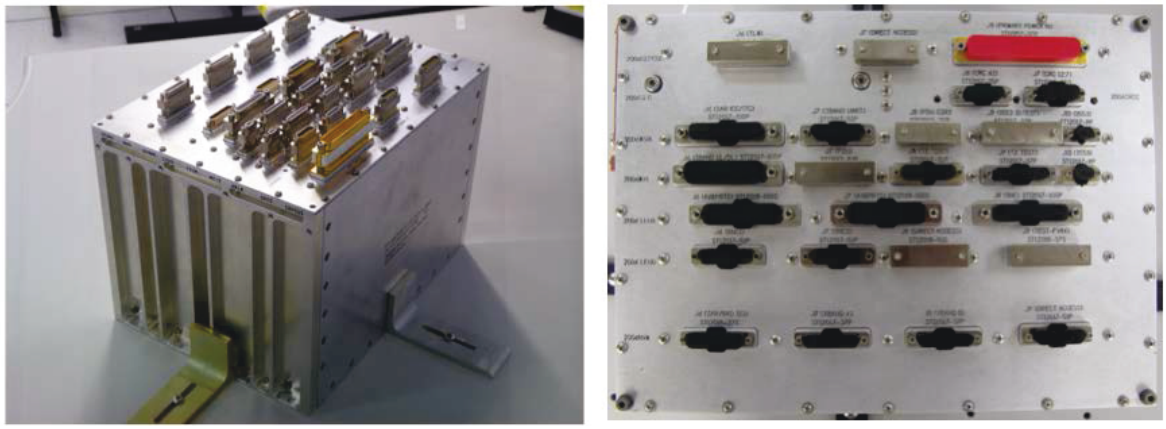

Figure 19. Example of pedestals for the connectors on the C&DH assembly as well as a cover plate to seal the gaps between faceplates of the individual cards in the box.

SMAP added other provisions to address EMC including a cabling design that assures a continuous Faraday cage between electronics boxes using twisted wire pairs with a shielded jacket (TPSJ). Jacket testing showed that TPSJ with Laird tape provides better shielding at L-band than TPSJ with copper braid overwrap. Because radiated emissions can be directional and connectors are often a source, the ICE was configured so that the connectors pointed away from the reflector to further attenuate emissions that could reflect interfere with science instruments. The BAPTA was identified by modeling to be a likely source of leakage; therefore, the observatory structure above the BAPTA was designed as a Faraday cage and the rotation pathway for emissions was directed into the spacecraft interior where any emissions would less likely interfere with science measurements.

Existing inherited designs (most of the commercial space assemblies used on SMAP) are being accepted without additional modifications for EMC. EMC requirements were levied on these assemblies but with the recognition some may be found non-compliant. In these cases, SMAP will use traditional EMI/EMC control techniques during integration and test in order to control emissions (adding EMI tape or cloth to cover possible areas of leakage).

9. Instrument Antenna Control

SMAP's attitude control and pointing system performs the key on-orbit operations needed to implement the conical scanning scheme employed for data acquisition by the radar and radiometer. The observatory uses a zero momentum bias, dual-spin architecture to rotate its large antenna at a spin rate of 13–14.5 rpm, while the spacecraft bus provides a three-axis controlled platform that maintains both itself and the instrument section's spin axis in a nadir-pointed orientation. The major pointing and control functional aspects and design characteristics are illustrated in Figure 20. A key challenge with the spinning antenna stems from its large spin axis moment of inertia, which at almost 240 kg-m^2 is larger than that of the spacecraft bus at about 190 kg-m^2.

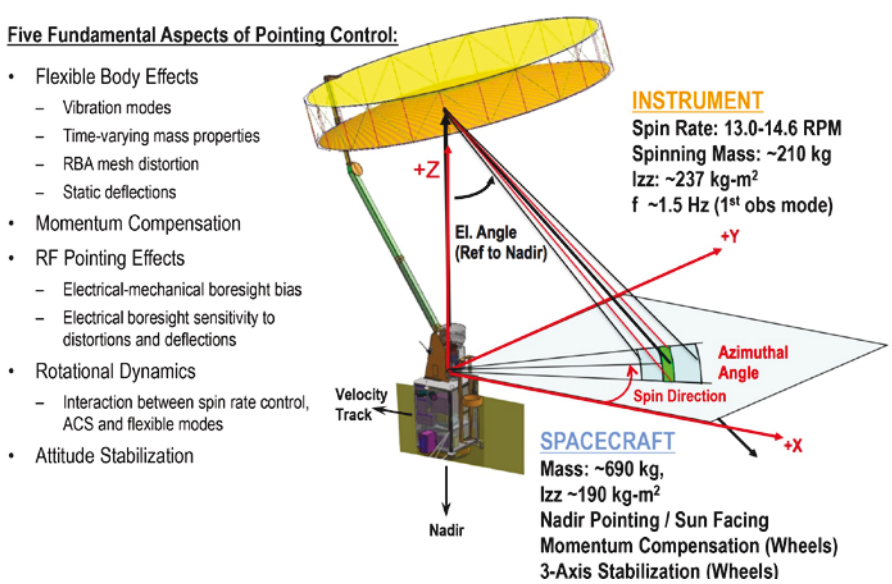

Figure 20. SMAP pointing and control system functional aspects and design characteristics.

Figure 21 shows the sensor and actuator suite and locations. This control system configuration was informed by a prior design concept for the Navy Remote Ocean Sensing System (NROSS) satellite, [20] which would have employed a similar sized-rotating antenna and nadir-pointing scheme (NROSS development was halted after Preliminary Design Review in the 1980s). From a control standpoint, SMAP took an integrated approach to momentum management, with momentum compensation for the spun side and three-axis control accomplished with a single set of four Reaction Wheel Assemblies (RWAs), rather than using a dedicated momentum wheel for spun-side momentum compensation. In a recent operational example of a nadir-pointing observatory employing a momentum-compensated rotating antenna, WindSat/Coriolis, a dedicated momentum wheel was also used to counteract the antenna's angular momentum, in a manner similar to that planned for NROSS [21]. SMAP's approach provides a degree of functional redundancy for wheel failure and reduces control complexity.

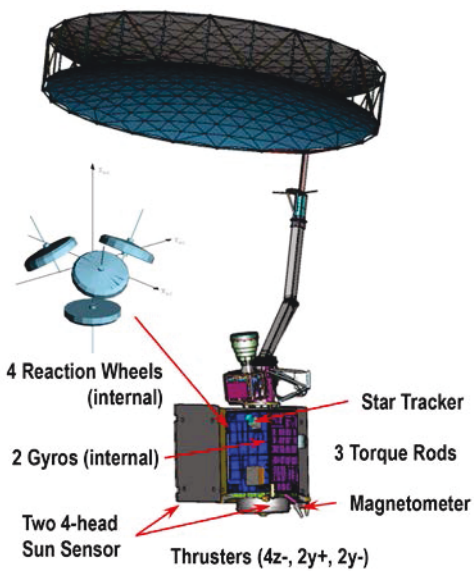

Figure 21. Observatory sensor and actuator description.

Figure 22 shows the system architecture, encompassing the attitude and spin rate determination functions, attitude control modes for both RWA and Reaction Control System (RCS) based three-axis control, spun-side momentum compensation, and the torque rod-based scheme employed for RWA momentum management. For translational maneuvers (needed for orbit altitude maintenance) and select contingency scenarios, the RCS is used due to the much larger control authority offered by the thrusters. For nominal mapping operations, this system can control nadir pointing errors due to precession and nutation to within 0.5 deg, with a stability tolerance of ±0.3 deg (3σ) [22].

From a design and verification standpoint, the key challenge for pointing and control is accommodating the flexible modes, especially for the large antenna and its supporting boom, while simultaneously controlling the antenna spin rate and nadir orientation to within the required tolerances. This has been accomplished via careful engineering of the primary frequencies associated with these various elements, to ensure adequate separation and avoid the potential for interference or undesired resonance effects. Frequency distribution of these system components is shown in Figure 23 to illustrate this aspect of the design. The minimum 1st flexible mode frequencies of the solar array, as well as the antenna and boom, became key design requirements on the structure to ensure adequate separation from the spin control system and the observatory's attitude control bandwidth.

10. Launch Vehicle Challenges

The launch vehicle selection process for SMAP involved both programmatic and technical challenges to develop an observatory design that was compatible with several potential medium- and large-class launch vehicles and to accommodate a launch vehicle selection late in the design lifecycle without stretching the development schedule or delaying the launch ready date. SMAP's strategy effectively isolated the observatory design from launch vehicle

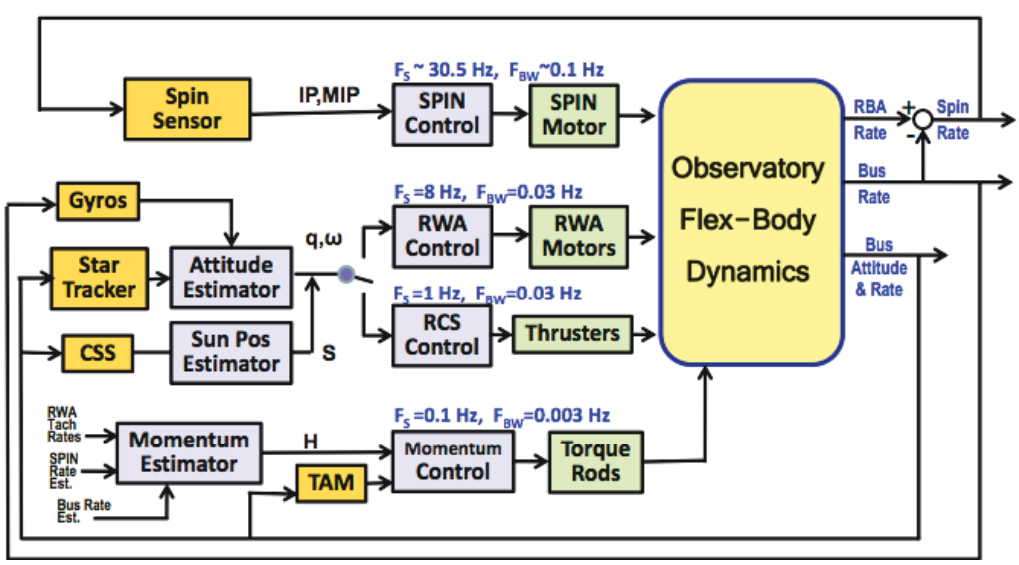

Figure 22. Pointing and control system architecture.

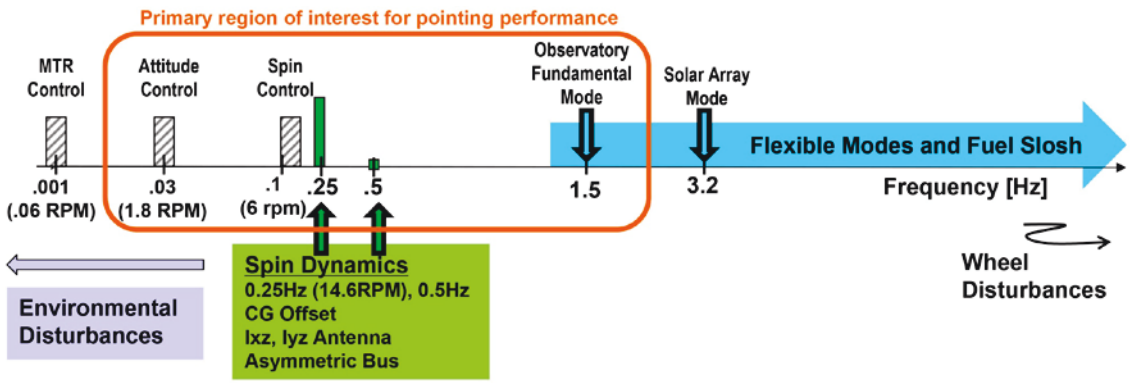

Figure 23. Frequency separation is the key to meet stability and performance requirements while not responding to disturbances.

uncertainty by applying very conservative bounding design loads and environments, designing to the most constraining fairing volume, and by developing a flexible launch vehicle adapter design to address vehicle-specific interface and mission design differences after launch vehicle selection.

When SMAP began Formulation in September 2008, there was a dearth of suitable, affordable medium-class launch vehicles commercially available [23]. SMAP was too massive to be lofted on a Taurus XL. Delta II production had been halted. The Falcon 9 had not yet flown. Evolved expendable-class launch vehicles (EELVs) were costly and grossly over-capable for SMAP, and SMAP's tall stowed configuration effectively eliminated it as a co-manifest option on an EELV. The situation was further complicated because NASA's Launch Services Program (LSP) was transitioning to a new launch services contract (NLS-2); there was uncertainty when the new contract would be in place and which vehicles would be initially available in the timeframe SMAP expected a launch vehicle selection.

The Project also simultaneously explored whether a partnership with the DOD Space Test Program (STP) could be formed wherein the DOD would provide launch services for SMAP. Several DOD agencies have high interest in using SMAP data in their applications [3] and were strong advocates to the STP for such a partnership. Under such a partnership, the DOD might have earlier access to critically needed soil moisture and freeze-thaw data to support their applications and NASA would realize a substantially lower mission cost. STP has occasional access to EELVs and more frequent access to Minotaur IV vehicles. The Minotaur IV uses components with a significant flight heritage such as surplus Peacekeeper stages, a Taurus fairing and attitude control system, and a mix of Minotaur I, Pegasus, Taurus, and other Orbital Sciences standard avionics and software [24]. The use of surplus Peacekeeper stages means the vehicle was defined by NASA to be a non-commercial launch system under the Commercial Space Act and therefore, it is not available for NASA acquisition. The Act allows for Minotaur use by DOD under certain circumstances that appeared potentially allowable for SMAP under a DOD partnership. The Minotaur IV had not yet flown at that time, but it appeared to be a good potential match for SMAP. The potential cost benefit to NASA of a DOD partnership was substantial, especially given the uncertainties in the commercial acquisition process, and for a time, the DOD partnership track seemed like the most likely prospect for a launch vehicle for SMAP. For these reasons, SMAP strove to develop an observatory that maintained Minotaur IV+ compatibility (the "+" variant replaces the Orion 38 upper stage with a Star 48 which provides more lift capability).

This was the launch vehicle context and design approach in which SMAP proceeded through its preliminary and then detailed final design until CDR in July 2012, when NASA announced selection of a Delta II launch vehicle for SMAP.

Persistent launch vehicle uncertainty drove SMAP towards mission and observatory designs that maintained compatibility with several launch vehicles: Minotaur IV+, Atlas V, Falcon 9 and then later the Delta II when it was on-ramped onto NLS-2 in October 2011. In most aspects, the Minotaur IV+ represented the most constraining vehicle choice. The largest drivers were its 92-in fairing, and its lift capability constraint and non-restartable upper stage, which limited its final orbit insertion capability for SMAP.

Typically in early formulation before launch vehicle selection, missions employ enveloping and highly margined design environments for compatibility with likely launch vehicles. Launch vehicle selection is typically completed by mission PDR so that as the observatory enters the final design phase, expected launch load requirements decrease around the selected vehicle and maturing coupled loads and mission analyses. The easing of requirements allows fewer design iterations (margin is 'cashed in' to address problems that arise in the detailed design). On SMAP, the early conservative and highly margined loads environment persisted through the entire design lifecycle, which in turn drove more design iterations to insure the design was compatible with the higher loads cases.

The 92-in fairing constraint significantly drove the observatory packaging to achieve a compact design. The spacecraft bus underwent several design iterations to package avionics, power, and radar electronics designs as the associated electronics packaging designs matured, while also accommodating commercial space assemblies for other

subsystems [transponders, transmitters, miniature inertial measurement unit (MIMUs), the large RWAs, etc.). The bus packaging also needed to accommodate an 80-kg propellant tank to support the mission design. The packaging requirements contributed to decisions to develop the NVM slice within the C&DH to avoid having to accommodate a separate solid state data recorder assembly. Harness design was a challenge to accommodate difficult bends and close clearances. The structure design was also optimized to reduce mass to insure healthy margins against the Minotaur IV+ lift capability. The spacecraft structure was designed with 7050 aluminum alloy and the structure includes a number of machined cutouts and thin walls that are time-consuming to fabricate. Thermal control was also a challenge in such a small bus due to the power dissipations (~1400 W). A passive thermal control approach was implemented for reliability and reduced complexity; but nearly every available exterior surface is used as a radiator.

Perhaps most significantly impacted by the 92-in fairing constraint were the stowed RBA and solar array packaging. The RBA has been the most sensitive assembly to launch vehicle uncertainty, undergoing several design iterations to address stowed packaging and launch loads, and thermal design iterations to address evolving launch phase mission design scenarios. The RBA along with the spin assembly is so intimately coupled to the observatory's fundamental architecture that these contracts were initiated early in Phase A; however the RBA is now the last flight assembly to be delivered to observatory integration and test, less than one year before launch, because the start of flight manufacturing was delayed until the design work could be stabilized and confirmed for the selected launch vehicle.

The solar array design was also driven by the 92-in fairing constraint. Unusually, SMAP's solar array has no exposed cells when stowed. Because of the small bus size, the adjacent sizes of the spacecraft to the solar array central panel are 'busy' and close clearances to the fairing envelope would not allow for a 'wrap around' solar panel stowage approach. The solar array folds over on itself, placing the outboard cells facing inward. This feature places high emphasis on ensuring there are robust battery energy margins available to accommodate solar array deployment contingencies following launch vehicle separation.

The mission design for orbit insertion was also developed initially around the Minotaur IV+ vehicle capability. The Minotaur IV+ upper stage is not restartable and to accommodate disposal requirements, the initial target specification placed the upper stage/observatory in an elliptical orbit (566 x 664 km). This provided for upper stage disposal within the required 25-year timeframe, but drove the spacecraft propulsion system to accommodate the additional delta V (and propellant capacity) to reach the final science orbit (685 km). This elliptical insertion orbit and delta-V strategy also enabled the maximum achievable dry mass on-orbit for the observatory, subject to the need for 80-kg propellant tank capacity on board the spacecraft.

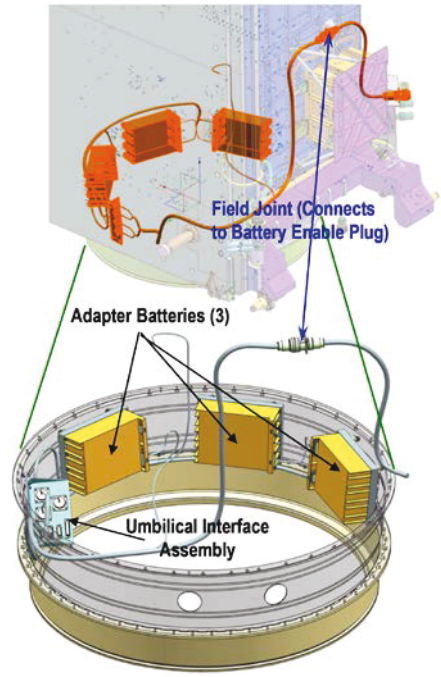

Figure 24. SMAP's launch vehicle adapter design accommodates changes needed for late launch vehicle selection.

To accommodate the Delta II selection, the existing Launch Vehicle Adapter (LVA) design was significantly modified to conform to Delta II mechanical and electrical interfaces (Figure 24). Because of the additional lift capacity of the Delta II and because the Delta II upper stage is restartable, the mission design was adapted to directly inject SMAP into its final science orbit. Additional secondary batteries were added to the LVA to provide appropriate power margins during the longer coast phase until separation and solar array deployment places the spacecraft is on internal power (Minotaur IV+ injection time was 16 minutes, Delta II is 60 minutes).

The Delta II has significantly increased mass and fairing volume resources than the Minotaur IV+; unfortunately, when the Delta II was selected, the SMAP design was mature and many subsystems were well into fabrication. It was not cost effective to iterate through another design cycle to take advantage of the additional resources. The added design and development effort to remain compliant with the Minotaur IV+ have ultimately allowed SMAP to accommodate a late launch vehicle selection without stretching out the development schedule or launch ready date, thereby allowing SMAP to retain its October 2014 launch ready date despite the launch vehicle uncertainty.

11. Lessons Learned

SMAP has significantly benefited from the experience and lessons from Aquarius and SMOS for the science measurements and instrument design, and from MSL for the avionics and power subsystem architectures. Personnel from these predecessor missions were engaged early in SMAP's

development so that their insight and lessons learned could be integrated into the early architectural design stages.

Key lessons learned from SMAP include:

(1) Coordinate science radar operating frequencies and planned scenarios very early with regulatory functions and key stakeholders. Spaceborne L-band science radars operate as secondary users within their allocated spectrum. The primary users, civil and defense aircraft terrestrial navigation systems, are increasingly wary about potential interference from secondary users. SMAP conducted significant analysis and testing to demonstrate very low interference risk potential and coordinated the results with these users early. SMAP made significant modifications to the radar design and operating approach to effectively eliminate risk of interference to primary spectrum users.

(2) Select the launch vehicle early; this is particularly important for new observatory designs where the number of design iterations can be driven by assumed constraints and conservative bounding environments (especially if they persist into detail design). Development effort on SMAP was impacted by the number of design iterations (packaging, repackaging to remain within fairing envelope, for instance), analysis cycles and thermal design iterations, and mission design iterations to accommodate various launchers before a final launch selection was made. This was unavoidable for SMAP given SMAP's launch vehicle and other circumstances.

(3) Integrated observatory design–spacecraft and instrument–SMAP is a highly integrated design that uniquely leverages spacecraft capabilities to simplify instrument design and operation. This resulted in lower overall design complexity and has also allowed for a more reliable design by reducing the number of possible major failure modes.

(4) Avoiding unnecessary complexity creep is a challenge in Formulation as new design insights incrementally unfold and thereby often reveal new issues to be resolved within the design. Occasional team 'resets' were imposed to reassess local requirements and design complexity within the context of the overall observatory design. These 'resets' often resulted in significant simplification and in reduced development risk and uncertainty.

(5) Realistically identify development challenges early and apply resources to mature these design areas, and qualify critical essential electronics parts and subassemblies to reduce downstream risk. SMAP successfully did this, aggressively applying resources to radar, radiometer, avionics, spin/dynamics and control, and the RBA–the key development challenges for the mission. As described earlier, the RBA and spin assemblies' designs were fundamental to the architectural definition and to enabling preliminary design to proceed, so these were selected early in Formulation and placed under contract. This reduced subsystem architectural- and system-level redesign cycles that can set back progress.

12. CONCLUSION

The SMAP observatory has been carefully designed to address a number of unique challenges posed by the mission objectives:

- Achieving global coverage every 2–3 days with a single instrument and observatory
- Achieving both high resolution and high soil moisture accuracy
- Minimizing data loss or corruption from L-band terrestrial RFI
- Using a deployable mesh reflector for L-band radiometric measurements
- Mechanical packaging of the large instrument antenna and spacecraft, with its associated structural design compatibility with several small-to-medium class launch vehicles and to accommodate a relatively late vehicle selection without delaying launch.
- Fault protection approach to minimize science measurement on-orbit down-time
- Adapting planetary heritage avionics to an Earth science mission application
- Design for EMC to avoid L-band emissions that could degrade science measurements
- Dynamics and pointing control of a large deployable spinning reflector

The design ensures that SMAP will provide high-quality science data.

REFERENCES

[1] "Earth Science and Applications from Space: National Imperatives for the Next Decade and Beyond," *Committee on Earth Science and Applications from Space: A Community Assessment and Strategy for the Future,* National Research Council, The National Academic Press, 2007. ISBN-10: 0-309-14090-0, ISBN-13: 987-0-309-14090-4.

[2] JPL SMAP website: http://smap.jpl.nasa.gov.

[3] Entekhabi, D., E. Njoku, P. O'Neill, K. Kellogg, et al., "The Soil Moisture Active Passive (SMAP) Mission," *Proceedings of the IEEE*, vol. 98, no. 5, May 2010.

[4] Spencer, M., K. Wheeler, C. White, R. West, J. Piepmeier, D. Hudson, and J. Medeiros, "The Soil

Moisture Active Passive (SMAP) Mission L-Band Radar/Radiometer Instrument," IEEE International 2010 Geoscience and Remote Sensing Symposium (IGARSS).

[5] Camps, A., J. Gourrion, J. M. Tarongí, A. Gutiérrez, J. Barbosa, and R. Castro, "RFI Analysis in SMOS Imagery," *Proceedings of the 2010 IEEE International Geoscience and Remote Sensing Symposium*, Honolulu, HI, USA, July 2010, pp. 2007–2010.

[6] Ruf, C., D. D. Chen, D. Le Vine, P. Matthaeis, and J. Piepmeier, "Aquarius Radiometer RFI Detection, Mitigation and Impact Assessment," *Proceedings of the 2012 IEEE International Geoscience and Remote Sensing Symposium,* Munich, Germany, July 2012.

[7] Bradley, D., C. Brambora, M. E. Wong, et al., "Radio-Frequency Interference (RFI) Mitigation for the Soil Moisture Active/Passive (SMAP) Radiometer," Geoscience and Remote Sensing Symposium (IGARSS), 2010 IEEE International, July 2010.

[8] Chan, S., M. Fischman, and M. Spencer, "RFI Mitigation and Detection for the SMAP Radar," Geoscience and Remote Sensing Symposium (IGARSS), 2011 IEEE International, July 2011.

[9] Spencer, M., S. Chan, E. Belz, J. Piepmeier, P. Mohammed, and J. Johnson, "Radio Frequency Interference Mitigation for the Planned SMAP Radar and Radiometer," Geoscience and Remote Sensing Symposium (IGARSS), 2011 IEEE International, pp. 2440–2443.

[10] Jones, C., et al., "Analysis of Potential Interference from SMAP Radar Transmissions into FAA ARSR-3, ARSR-4, and CARSR Radars in the 1215–1300 MHz Band and Interference Avoidance Strategies," Jet Propulsion Laboratory internal document.

[11] Huneycutt, B., S. Hensley, G. Purcell, et al., "Test Report on the Effects of Pulsed Interference from L-band Spaceborne and Airborne Radars on GPS L2 Receivers," Jet Propulsion Laboratory internal document, Nov. 1, 2010.

[12] Sanders, F., et al., "NTIA Study regarding EMC between Proposed NASA SMAP Orbital Radar System and FAA ARSR Systems," NTIA/ITS.

[13] Mobrem, M., S. Kuehn, C. Spier, and E. Slimko, "Design and Performance of Astromesh Reflector Onboard Soil Moisture Active Passive Spacecraft," IEEE 2012 Aerospace Conference, March 2012.

[14] Mohammed, P., SMAP L1B Radiometer Data Product Algorithm Theoretical Basis Document, GSFC.

[15] Spencer, M. W., C. W. Chen, H. Ghaemi, S. F. Chan, and J. E. Belz., "RFI Characterization and Mitigation for the SMAP Radar," TGARS, to be published.

[16] West, R., SMAP L1 Radar Data Products Algorithm Theoretical Basis Document, Jet Propulsion Laboratory.

[17] Heidecker, J., M. White, M. Cooper, D. Sheldon, F. Irom, and D. Nguyen, "Qualification of 128 Gb MLC NAND Flash for SMAP Space Mission," Integrated Reliability Workshop Final Report (IRW), 2010 IEEE International, Oct. 2010.

[18] Heidecker, J., "NAND Flash Screening and Qualification Guideline for Space Application" JPL Publication 12-1, Jet Propulsion Laboratory, Pasadena, CA, 2012.

[19] Newson, S. L., and C. H. Huang, "SMAP Electromagnetic Compatibility (EMC) Design Control Plan," Jet Propulsion Laboratory Internal Project Document, April 14, 2010.

[20] Mak, P. H., "Pointing and Stabilization Issues of Large Spinning Antennas," *Proceedings of IEEE Position Location and Navigation Symposium*, Navigation into the 21st Century, IEEE Plans, pp. 230–235, 1988.

[21] Gaiser, P. W., K. M. Germain, and E. M. Twarog, "WindSat—Spaceborne Remote Sensing of Ocean Surface Winds," *Proceedings of IEEE Oceans Conference,* vol. 1, p. 280, 2003.

[22] Alvarez-Salazar, O. S., D. Adams, M. Milman, R. Nayeri, S. Ploen, L. Sievers, E. Slimko, and R. Stephenson, "Precision Pointing Architecture of SMAP's Large Spinning Antenna," IEEE 2010 Aerospace Conference, Big Sky, MT, to be published.

[23] "Review of NASA's Acquisition of Commercial Launch Services," NASA Office of Inspector General, February 17, 2011.

[24] "Minotaur IV Users Guide," Release 1.1, Orbital Sciences Corporation, January 2006.

BIOGRAPHIES

Kent Kellogg *received a B.S. in Electronic Engineering from California Polytechnic State University, San Luis Obispo in 1983. He joined JPL's Spacecraft Antenna Group in 1983 and is currently SMAP Project Manager. His prior roles include managing JPL's Telecommunication, Radar and Tracking Division, Spacecraft Telecommunications Equipment Section, SeaWinds/ QuikSCAT Instrument and Project and supervising JPL's Spacecraft Antenna Group.*

Dr. Sam Thurman *received B.S., S.M., and Ph.D. degrees in Aerospace Engineering from Purdue University (1983), Massachusetts Institute of Technology (1985), and the University of Southern California (1995), respectively. He jointed JPL in 1987 and is currently the SMAP Deputy Project Manager. His prior roles include Deputy Manager of JPL's Autonomous Systems Division, and several system engineering and management assignments in the Mars Exploration Program. Before joining JPL, he worked as a missile guidance analyst at the Charles Stark Draper Laboratory in Cambridge, Massachusetts.*

Wendy Edelstein *received her B.S. degree in Electrical Engineering with minor in Applied Mathematics from the University of California, San Diego in 1988. She joined JPL in 1988 and is currently the SMAP Instrument Manager. Her prior roles include Deputy Section Manager of the Radar Science & Engineering Section, Group Supervisor for the Advanced Radar Technology Group and radar technologist where her primary research interests included Transmit/Receive modules, RF component miniaturization and lightweight antenna technologies.*

Dr. Michael Spencer *received the B.S. degree in Physics from the College of William and Mary, the M.S. degree in Planetary Science from The California Institute of Technology, the M.S. degree in Electrical Engineering from the University of Southern California, and a Ph.D. in Electrical and Computer Engineering from Brigham Young University. He joined JPL in 1990 and has served as the SMAP Instrument System Engineer. He is currently the Deputy Manager of JPL's Radar Science and Engineering Section; he is also the SMAP Instrument Scientist.*

Dr. Gun-Shing Chen *received the B.S. degree in Mechanical Engineering from Cheng-Kung University, Taiwan in 1977; an M.S. degree in Aerospace Engineering from University of Texas at Austin in 1981; and a Sc.D degree in Aeronautics and Astronautics from Massachusetts Institute of Technology in 1986. He joined JPL's Structures and Dynamics Research Group in 1986 and is currently the SMAP Flight System Manager. His prior roles include Group Supervisor, Section Manager, Assistant Division Manager in the Mechanical System Division, Chief Engineer and Assistant Division Manager in the Instruments and Science Data Systems Division, Mechanical Project Element Manager (PEM) for the Deep Space-1/Miniature Imaging Camera and Spectrometer (MICAS) and EOS Microwave Limb Sounder (MLS) Instrument Projects, Deputy Mechanical PEM for the Mars Exploration Rovers (MER) Project, and Instrument Manager for the Active Mirror Telescope (AMT) Project*

Dr. Mark Underwood *received a B.S. Engineering from UCLA in 1981 and Ph.D. in Chemical Engineering at the University of Pennsylvania in 1987. He joined JPL's Spacecraft Power Section in 1987 and is currently the SMAP Mission Assurance Manager and is responsible for safety, EEE parts, environments, reliability, software and hardware quality assurance. His prior roles include Group Supervisor for the Power Electronics and Systems Group and Manager of the Power Systems Section. Prior to joining SMAP, he was the Deputy Mission Assurance Manager for the Juno project.*

Shawn Goodman *received an M.S. in Mechanical Engineering from Rensselaer Polytechnic Institute. He joined JPL's Spacecraft Mechanical Engineering Section in 1991 and is currently SMAP Project System Engineer. His prior roles have included Group Supervisor, Deputy Section manager and Section manager of the Spacecraft Mechanical Engineering Section. He has worked a number of flight projects including MSTI, Sojourner, MGS, SIR-C, DS1, X2000, OPSP, MER, and MSL.*

Benhan Jai *received his Masters degree in Computer Engineering from the University of Southern California. He joined JPL in 1985 where he served in a number of engineering and management roles involving ground data system development, mission operations system development, and mission management. He is currently the SMAP Mission Systems Manager. His previous assignments have included the development of the Ground Data System and the Mission Operations System on many missions including NASA Scatterometer, SeaWinds, Mars Global Surveyor, Stardust, Mars Odyssey, and Mars Surveyor Operations Projects. Prior to joining SMAP, Ben led the development of mission operations and ground data systems of the Mars Reconnaissance Orbiter Project (MRO), and led the entire flight teams of the MRO through launch, cruise, MOI, and aerobraking to the completion of the primary science phase of the mission.*

Dr. Eni Njoku *received the B.A. degree in natural/electrical sciences from the University of Cambridge, U.K., in 1972 and the M.S. and Ph.D. degrees in electrical engineering from MIT in 1974 and 1976, respectively. He joined JPL in 1977 and he is currently the SMAP Project Scientist, a JPL senior research scientist, and also supervisor of the Water and Carbon Cycles Group. His prior roles have included managing JPL's Geology and Planetology Section and serving as discipline scientist for ocean and earth science data systems at NASA. His primary research interests are in developing microwave remote sensing techniques for land surface hydrology and climate. His current research includes microwave modeling, retrieval algorithm development, field experiments, and data analysis using radiometers and radars.*

ACKNOWLEDGEMENTS

The work described in this paper was carried out at the Jet Propulsion Laboratory, California Institute of Technology, under a contract with the National Aeronautics and Space Administration. Part of this work was also carried out at the NASA Goddard Space Flight Center.